Journal of Membrane Science 428 (2013) 507–515

Contents lists available at SciVerse ScienceDirect

Journal of Membrane Science

journal homepage: www.elsevier.com/locate/memsci

Substrate effect on the swelling and water sorption of Nafion nanomembranes

Graciela C. Abuin [a], M. Cecilia Fuertes [b], Horacio R. Corti [c,*]

[a] Centro de Procesos Superficiales, Instituto Nacional de Tecnología Industrial (INTI), Av. Gral. Paz 5445, B1650KNA, San Martın, Buenos Aires, Argentina
[b] Gerencia Química, Comisión Nacional de Energía Atómica (CNEA), Av. Gral. Paz 1499, B1650KNA, San Martín, Buenos Aires, Argentina
[c] Departamento de Física de la Materia Condensada, Comisión Nacional de Energía Atómica (CNEA), Av. Gral. Paz 1499, B1650KNA, San Martín, Buenos Aires, Argentina

ARTICLE INFO

Article history:
Received 1 September 2012
Received in revised form
28 October 2012
Accepted 29 October 2012
Available online 16 November 2012

Keywords:
Nafion
Nanofilms
Water sorption
Swelling
Aging
Substrate effect

ABSTRACT

Swelling and sorption of water, from the vapour phase, by thin (100–1000 nm) and ultra-thin (< 100 nm) Nafion nanomembranes deposited on several surfaces were determined using quartz crystal micro-balance and environmental ellipsometric porosimetry techniques. The water uptake at room temperature, measured as the number of water molecules per ionic group in the polymer, is much lower than that observed in bulky Nafion 117 membranes. Water sorption by supported nanofilms was found to be independent of film thickness, but it depends on substrate nature. Aging due to slow relaxation of the polymer microstructure is also discussed. Results are relevant for modelling the three-phase region of proton exchange membrane fuel cells, where a thin Nafion film covers the carbon supported catalyst nanoparticles.

1. Introduction

Nafion ionomers, the product of copolymerization of perfluorosulfonate vinyl ether and tetrafluoroethylene, is the most used proton exchange membrane (PEM) in PEM fuel cells as well as in electrolysers and other electrochemical devices. Consequently, the properties of this commercial polymer have been extensively studied for decades and many of them are now well established [1]. Nevertheless, the microstructure of hydrated Nafion is still controversial.

The cluster-network model for the microstructure of wet Nafion, proposed by several authors since the early 1980s, [2–6] consider the swelled polymer as a network of ionic cluster formed by the sulphonic groups arranged as inverted micelles, around 4 nm in diameter, interconnected through narrow water channels, around 1 nm in diameter. However, a recent simulation of former small-angle X-ray or neutron scattering (SAXS/SANS) data of Nafion [7] seems to indicate that the structure of the hydrated polymer correspond to that of inverted-micelle cylinders forming water channels 2.4 nm average in diameter.

The performance of PEM fuel cells is largely determined by the structure of the membrane electrode assembly (MEA), more specifically, by the molecular architecture of the three-phase region, that is, the space where merge the metallic catalyst (usually Pt nanoparticles supported on carbon), the PEM, and the gases (H_2 in the anode side and O_2 in the cathode side) [8].

The three-phase region is not limited to the catalyst layer in direct contact with the PEM, since a Nafion binder is used in the preparation of the MEA in order to form a percolated network of PEM around all the catalyst particles. Therefore, the structure of the three-phase region depends on the method of preparation of the catalyst layer and the MEA, which can be performed through two basic procedures. In the PTFE-bonded method the platinum catalyst supported on carbon (Pt/C) is mixed with a polytetrafluoroethylene (PTFE) emulsion as binding material, dried, baked at high temperature, and finally impregnated with 5 wt% Nafion solution (2 mg cm^{-2}). The electrodes are bonded to the polymer electrolyte membrane through hot pressing to complete the MEA [9,10]. In the thin-film method the binding material in the catalyst layer is only Nafion, as the membrane. A 5 wt% Nafion solution is mixed with 20 wt% Pt/C supported catalyst in a ratio of 1:3 Nafion/catalyst and added to a water–glycerol mixture in order to prepare an ink, which is applied on both side of the membrane to form the MEA [11,12]. Alternatively, the catalyst layer can be applied by casting on a PTFE blank, and then decaled on the membrane [13].

In the first case the thickness of the Nafion film deposited on the Pt/C catalyst is around 500 nm, but it can be thinner in the final MEA after hot pressing. In the thin-film the binder distributes homogeneously over the entire surface of the Pt/C catalyst

* Corresponding author. Tel.: +54 11 6772 7174; fax: +54 11 6772 7121.
E-mail address: hrcorti@cnea.gov.ar (H.R. Corti).

0376-7388/$ - see front matter © 2012 Elsevier B.V. All rights reserved.
http://dx.doi.org/10.1016/j.memsci.2012.10.060

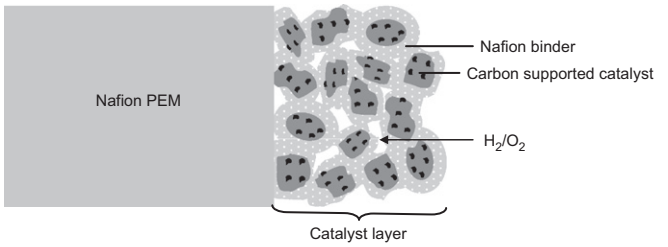

Fig. 1. Non-scaled scheme of one side (cathode or anode) of a MEA showing the three-phase region. The thicknesses of the Nafion membrane and catalyst layer are usually 50–170 μm and 1–5 μm, respectively. Pt nanoparticles (black dots) are typically 2–5 nm in size, and Vulcan carbon aggregates (gray forms) have sizes around 100 nm.

and, assuming a surface area of around 250 $m^2\,g^{-1}$ as that reported for Vulcan carbon, [14] the thickness of Nafion film is expected to be slightly over 1 nm. However, this value can be considered as a lower bound because the surface area of the supported Pt/C catalyst could be reduced due to the aggregation of the carbon particles during the Pt reduction, and because of heterogeneities in Nafion distribution. Fig. 1 shows schematically the Nafion distribution in the three phase regions of the MEA. Roughly, the expected thickness of the Nafion film covering the catalyst particles can fluctuate from few nm up to 500 nm.

The properties of Nafion nanofilms covering catalyst-support surfaces, as in the three-phase region, have been approached recently from both, the experimental and theoretical view. Thus, Markovic and coworkers [15] studied the adsorption of thin layers of Nafion on Pt(1 1 1), Pt(1 1 0), Pt(1 0 0) and polycrystalline platinum surfaces and proposed a model to account for the irreversible adsorption of the sulphonate anion. Franco et al. [16] developed a multiscale model with the aim of explaining the inhibition of the oxygen reduction reaction (ORR) on Pt electrodes with adsorbed Nafion. Ohma and coworkers have studied the ionomer and water adsorption on carbon supports using molecular dynamics simulations [17], multi-scale modelling and experimental analysis [18] in relation to the reduction of platinum loading in the catalytic layer of PEM fuel cells. Recent coarse-grained molecular dynamics studies reveal that the amount and distribution of Pt in the catalyst layer and the carbon morphology have a pronounced effect on the Nafion nanofilm structure [19,20].

Water uptake by Nafion nanofilm covering the Pt/C catalyst is expected to be determined by its structure and, in turn, influences other relevant properties of the film, such as proton conductivity [21,22]. While water uptake of bulk Nafion membranes (typically Nafion 117, 178 μm thickness) in the acid form has been measured by several authors from the vapour [23–34] and the liquid phase (water activity, $a_w=1$) [27,34–36] at temperatures between 20 and 30 °C, the information referred to water sorption in thin Nafion membranes is scarce and all of it was obtained using Quartz Crystal Microbalance (QCM) technique.

The first study of water sorption by Nafion membranes using QCM was performed by Krtil et al. [37] on thin films (20–80 nm) prepared by casting at 25 °C and they reported water uptakes similar to those of the bulky membranes for all the water activities. Yamamoto et al. [38] determined the water sorption at 50 °C by a Hyflon Ion thin membrane (1.5 μm) obtained by casting, and reported a water uptake much lower than that both, the bulky Hyflon Ion and a bulky Nafion membrane. More recently, Kongkanand [39], also using QCM, measured water sorption of Nafion films with thickness between 33 and 3000 nm, observing that the water uptake for different film thicknesses was similar for Nafion films thicker than 500 nm, but for thinner films slightly lower water contents were observed specially at high water activities.

In summary, the results of water sorption by very thin Nafion and Nafion-like membranes using QCM are contradictory and were obtained for films deposited on the gold surface of QCM.

The main objective of this work is to perform a comprehensive study of water sorption and swelling properties of casted Nafion nanofilms of variable thickness, supported on different solid surfaces, using QCM and environmental ellipsometric porosimetry (EEP) techniques. The use of a novel alternative technique, such as EEP, for very thin films will allow us to compare the water sorption of the films deposited on different kind of substrates with that of unsupported bulky Nafion membranes used in PEM fuel cell MEAs. The water uptake by Nafion thin films, as those covering the catalyst particles in the three-phase region, is relevant for molecular models describing the transport properties in the three-phase region, aiming to optimize the PEM fuel cell performance by means of molecular design using model parameters [16,18], as well as in other approaches using macroscopic parameters, like the ionomer/carbon ratio [40,41].

2. Experimental

The study of water uptake by supported thin Nafion membranes was performed by employing quartz crystal microbalance (QCM) and environmental ellipsometric porosimetry (EEP). In this section, we will briefly describe the features of both techniques.

2.1. Thin and ultra-thin Nafion film preparation

Nafion nanofilms, with thickness between 9 and 80 nm, for QCM measurements were deposited over a quartz crystal (ICM 151218–10, gold electrode) previously cleaned with an acetone soaked cotton hyssop. The solutions used for depositing ultra-thin membranes over the crystal by casting or spin coating were prepared by mixing a known volume of a Nafion solution (Ion Power, LQ-1115 15% w/w Nafion 1100 EW) with methanol.

In the case of films prepared by casting, the area of the film was limited by an o'ring compressed by a PTFE ring fixed by a steel piece, as shown in Fig. 2. A known volume of solution containing 50 μg of Nafion per cm^3 was poured in the space limited by the o'ring, and the solvent was then evaporated at

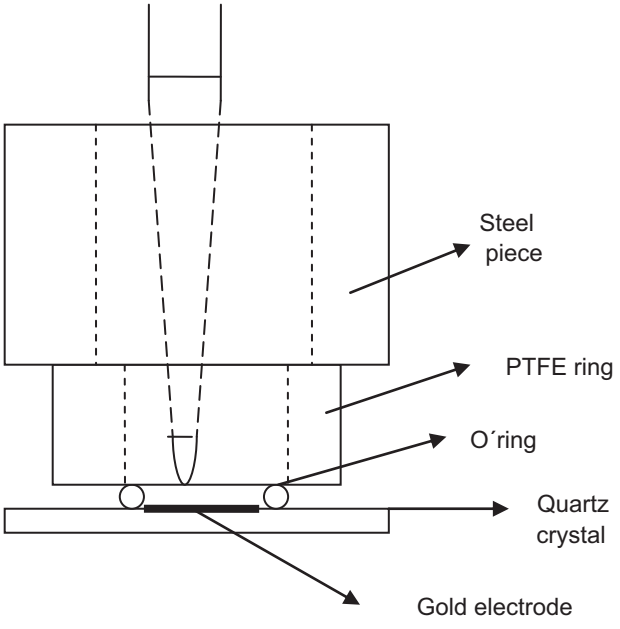

Fig. 2. Scheme of the setup to deposit ultra-thin films onto a quartz crystal.

room temperature. The final membrane thickness was estimated from the area, considering that the density of recast Nafion is 1.8 g cm^{-3} [37]. Films with thickness around 80 nm were also deposited over the quartz crystal by spin coating using a commercial spin coater (Laurell, WS 650 Lite) at 3000 rpm during 30 s. The Nafion film deposited outside the sensitive area of the crystal was carefully removed with an acetone soaked cotton hyssop.

As a checking procedure, the thickness of the nanofilms deposited on the crystals was measured by AFM in contact mode using a Veeco–DI Multimode Nanoscope IIIa. The measured thicknesses were close to the estimated ones using the mass of Nafion deposited on the working area. The estimated thicknesses were reported in the results section because they correspond to average values on the entire area of the QCM.

The Nafion nanofilms for EEP measurements were deposited from Nafion solutions by spin coating on glass, indium tin oxide (ITO), silicon, gold, and graphite substrates. Membranes with thickness in the range 80–1000 nm were prepared by pouring over the whole substrate area a drop of known volume of 5 wt% Nafion solution diluted with methanol. All the substrates were previously cleaned with acetone, ethanol and finally dried with air. In the case of graphite the working surface was polished to 1000 grade before cleaning. Spin coating was performed on cleaned substrates at 3000 rpm during 30 s.

2.2. Quartz crystal microbalance

A QCM, described in detail elsewhere, [42,43] was used to measure the water uptaken by supported nanomembranes (9–80 nm in thickness) prepared by casting or spin coating over the quartz crystal. Once the solvent was evaporated and the membrane became rigid, the quartz crystal was mounted on the QCM holder contained within a sealed PTFE chamber under a dry nitrogen stream, to obtain the dry mass of the film. Once the equilibrium resonance frequency has been reached, the dry nitrogen was replaced by an air stream previously bubbled across saturated aqueous salt solutions at 25 °C, and the change in resonance frequency was measured. This procedure was repeated employing different saturated salt solutions, in order to measure water mass uptaken by the film in the range of water activity ($a_w = p/p_0$, p_0 being the saturation water vapour at the working temperature) from 0.33 to 1. The saturated solutions used to control the water activity were: $MgCl_2 \cdot 6H_2O$ ($a_w = 0.33$), $LiNO_3 \cdot 3H_2O$ ($a_w = 0.47$), NH_4NO_3 ($a_w = 0.62$), KBr ($a_w = 0.81$) and $BaCl_2 \cdot 2H_2O$ ($a_w = 0.92$). All the reagents analytical grade were used as received: $MgCl_2 \cdot 6H_2O$ (Merck), $LiNO_3 \cdot 3H_2O$ (Merck), NH_4NO_3 (Mallinkrodt), KBr (Merck) and $BaCl_2 \cdot 2H_2O$ (Mallinkrodt).

Nitrogen and humidified air flow rate were kept as low as possible, until a steady state resonance frequency was attained. It was found that QCM reading is modified by stream flow rate, in such a way that higher flow rate values led to higher film water uptake values.

The mass change upon sorption was calculated from the measured resonant frequency shift, Δf, by means of Sauerbrey's equation [44]:

$$\Delta f = \frac{2n{f_0}^2}{A\rho^{1/2}\mu^{1/2}}\Delta m \quad (1)$$

where n is the harmonic's order (usually $n=1$), $f_0 = 10^7$ Hz is the base frequency of the crystal, $A = 0.204$ cm^2 is the electrode area, $\rho = 2.648$ g cm^{-3}, and $\mu = 2.947 \times 10^{11}$ g cm s^2 are the density and shear modulus of the crystal, respectively.

Thus, the dry membrane mass, m_d, was obtained from the difference between the resonant frequencies of the naked and dry film covered quartz crystal. The mass of water, m_w, uptaken by the film was calculated from the difference between the resonant frequencies of the film equilibrated with water activity a_w, and the dry film.

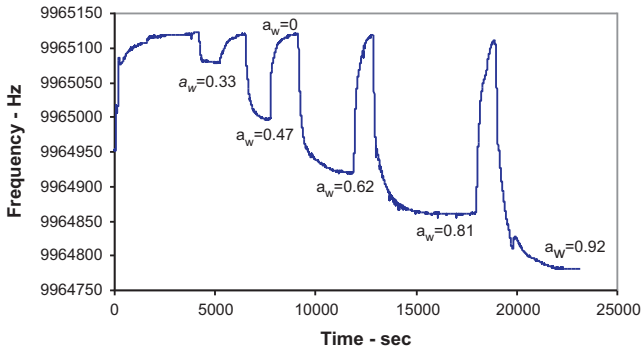

Fig. 3. Resonant frequency shift of the QCM for a thin Nafion film (80 nm.) exposed at different water.

Fig. 3 shows the time behaviour of the resonant frequency for a 17 nm membrane casted over the quartz crystal, exposed to humidified air streams of different water activities, including periods of dryness. It is worth to note that the sorption/desorption equilibrium is reached in time intervals of few minutes.

2.3. Environmental ellipsometric porosimetry

The precision of the water sorption measurements using QCM deteriorates when nanofilms were thicker than 100 nm. Therefore, the EEP technique was employed to measure the water uptake by Nafion nanomembranes of thickness between 80 and 1000 nm, using an environmental ellipsometric porosimeter (EEP, SOPRA GES5A).

The EEP technique, first reported by Baklanov and co-workers, [45] is a very powerful technique for studying the evolution of thickness and refractive index of supported porous thin films at different humidity conditions. The experimental device is based on the coupling of a pressure controlled chamber and a variable angle spectroscopic ellipsometer. Briefly, film thickness and refractive index values were obtained from the ellipsometric parameters Ψ and Δ [46] under nitrogen flux containing variable water activities from 0 to 1.

In porous films whose thickness does not change significantly during the water sorption (air inside the pores is replaced with water), water volume sorbed at each a_w value is determined by modelling the refractive index obtained according to an effective medium approximation. Sorption–desorption isotherms are then plotted using the water volume sorbed by the porous film at each a_w value [47–49].

In the case of a Nafion film, the change in thickness during water sorption as a_w increases is remarkable. In this work, thickness evolution will be used to calculate the water/Nafion mass ratio at each a_w, considering that the assumption of additivity of the volumes of dry Nafion and water is valid, as suggested by Morris and Sun [23] from the study of swelling of Nafion 117 as a function of the water content. Recently, Benziger and coworkers [50] performed a detailed study of the linear swelling strain of Nafion and concluded that the excess volume per water molecule is large for the first four water molecules adsorbed, and it remains very low at higher water contents. In fact the swelling strain calculated assuming zero excess volume of mixing agrees with the experimental results within the experimental error at $a_w > 0.2$.

In order to relate membrane thickness with water content using the volume additivity assumption the density of dry Nafion

in H^+ form is required. This is not a trivial issue since densities of unheated recast membranes were found to be 20% lower in water than that of commercial Nafion membranes and recast membranes heated above 120 °C [51,52]. Thus, for an acid treated recast membrane with a volume fraction of water equal to 0.33, the measured density [51] is (1.67 ± 0.14 g cm^{-3}), while the recast membrane heated one hour at 140 °C, recover the density of the commercial membrane (2.05 ± 0.17 g cm^{-3}), with a similar water volume fraction (≈ 0.10), although a lower density (1.90 ± 0.01 g cm^{-3}) for a dry Nafion 117 membranes has been reported [53].

The dry recast Nafion membrane density of 1.80 g cm^{-3}, reported by Paik et al. [54], was used by Krtil et al. [37] to calculate the thickness of thin Nafion membranes. On the other hand, if the additivity assumption is used along with the density reported for the unheated recast membrane, [51] a value of 2.00 g cm^{-3} is obtained for the dry film, that is, around 10% higher than that used in previous sorption studies using the QCM technique.

In this study we decided to adopt 1.80 g cm^{-3} for the density of dry Nafion and 1.00 g cm^{-3} for the density of pure water. The impact of this choice on the sorption properties of Nafion films measured with the EEP technique will be discussed in Section 3.2.

Nafion refractive index was determined from the ellipsometric data at $a_w=0$ using a Cauchy approximation for transparent materials [46,55]. The thicker films were selected to obtain more reliable data; then, the calculated optical constants were fixed in order to determine the thickness of thinner films. The equilibration time at each water activity was 20 s, while the measuring time was 10 s. No differences were observed for longer equilibration times (180 s).

For both techniques, QCM and EEP, the water uptake of the Nafion nanofilms was expressed by the number of water moles per exchange site mole (–SO_3H), λ, calculated as:

$$\lambda = \frac{m_w M_0}{m_d M_w} \tag{4}$$

where $M_w=18.016$ g mol^{-1}, and $M_0=1100$ g mol^{-1} are the water molecular weight and the Nafion equivalent weight, respectively.

3. Results and discussion

In the next sections we summarize the sorption and swelling characteristics of Nafion nanomembranes, of thickness between 17 and 1000 nm, supported on different substrates, using the QCM and EEP techniques. Before that it is important to analyse briefly the water sorption by bulky Nafion membranes and also the few results reported in the literature for thin Nafion recast films.

Water sorption from the vapour by Nafion 117 membranes are shown in Fig. 4 as the best fits of the data reported in the literature at 20 °C [28,31], 25 °C [23,25,29,30] and 30 °C [26,32,33]. Although the dispersion of the data at each temperature is large over all the range of water activities, the isotherms at 20, 25 and 30 °C almost overlap for $a_w > 0.4$ and exhibit the typical BET pattern. In the comparison with water sorption in thin films we will use the best fit of all the data in this temperature range.

For comparison with our results in thin Nafion films, only water sorption data from the vapour is shown in Fig. 4 because water uptake by Nafion from the liquid phase is higher than the water uptake from the vapour phase at $a_w=1$ [27,36]. This effect is known as Schroeder's paradox [56], and it seems to disappear when the membranes are pre-treated by vacuum drying at temperatures above 110 °C [34]. In Fig. 4 are also included

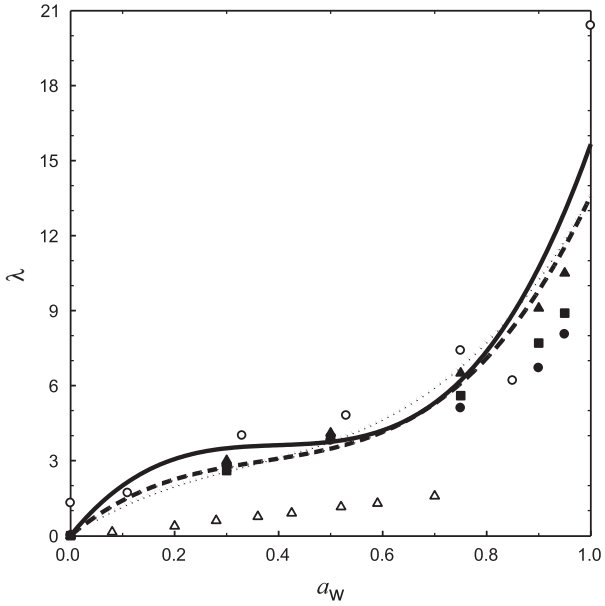

Fig. 4. Water sorption isotherm of Nafion 117 membranes and thin Nafion films determined by QCM. The lines correspond to the fit of the data for Nafion 117 at 20 °C (· · · · · · ·), 25 °C (——), and 30 °C (– – –). QCM data: (○) [37] ($\leq$80 nm); (Δ) [38] (1.5 μm); [39] (■) 30 °C (1 μm); (▲) 80 °C (1 μm); (●) 80 °C (33 nm).

previous results in thin Nafion membranes [37–39], in order to emphasize the discrepancies among the results obtained by different authors using the QCM technique.

The values of λ reported by Kritl et al. [37] are similar to those of the bulky membranes for all the water activities, as can be seen in Fig. 4. It is worth to note that the water uptake at $a_w=1$ is unusually high for sorption from the vapour phase and, unexpectedly, the sorption at $a_w=0$ is not null. The authors quoted that the water uptake determined with QCM was independent of the flow rate of humidified air when the flow was kept between 10 and 15 cm^3 s^{-1}, contrary to our finding, quoted in Section 2.2, that a high flow rate led to high water uptake values. Also Kongkanand [39] pointed out fails in the experiment by Kritl et al. [37] based on the observed very slow water uptake. The water uptake reported by Yamamoto et al. [38] for a Hyflon Ion thin membrane (1.5 μm thick) at 50 °C is much lower than that of a Nafion membrane 1 μm thick at 30 and 80 °C, as indicated in Fig. 4. On the other hand, the results by Kongkanand indicates that the water uptake of the membranes depends on their thickness, being lower than the values for the bulky membrane at high water activity, and the water uptake depression becomes more important for the thinner films.

3.1. Water sorption of ultra-thin (< 100 nm) Nafion membranes

The water uptake of ultra-thin Nafion films deposited on the gold surface of the quartz crystal and determined by QCM technique is depicted in Fig. 5a. The thickness of the cast prepared films range from 17 to 88 nm and the sorption of water does not seem to have a clear dependence on the film's thickness, although the water sorption of thinner films (17, 26, and 61 nm) is slightly lower than that of 80 and 88 nm films, especially at high water activities in agreement with the results by Kongkanand [39], who observed slightly lower water sorption on a 33 nm film compared with a film 180 nm in thickness at a higher temperature 80 °C than that used in this work.

Fig. 5a also shows the water uptake of a 75 nm Nafion film determined by EEP. The measurements were performed on a fresh

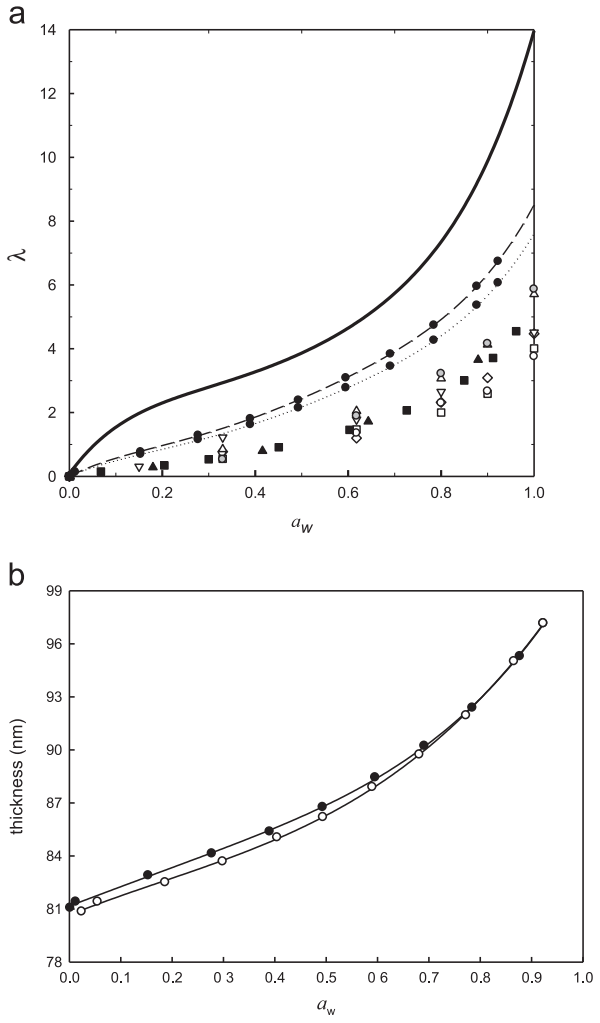

Fig. 5. (a) Water sorption isotherm at room temperature of supported ultra-thin Nafion films determined by QCM (open symbols) and EEP (filled symbols) as compared to bulky Nafion (solid line). Films supported on gold: (◇) 17 nm; (□) 26 nm; (○) 61 nm; (▽) 80 nm; (△) 88 nm; (■) 75 nm; (▲) 75 nm—10 days annealing. Film supported on PTFE: (◍) 66 nm. Film supported on glass: (●) 81 nm (dash and dotted lines correspond to isotherms calculated using dry Nafion density 1.80 g cm^{-3} and 2.00 g cm^{-3}, respectively); (b) Swelling of an ultra-thin Nafion film deposited on glass as a function of the water activity during the sorption (●) and de-sorption (○).

film and on a film annealed during 10 days. The results indicate that water sorption in this film is within the range of values of λ determined by the QCM technique for the 80–88 nm films.

The high dispersion is attributed to heterogeneities in the distribution of the nanoscopic polymer film on the substrate surface. The extended chain length of Nafion ($M_w \approx 2.10^5$ g mol^{-1}) is around 350 nm, but it forms rod-like hexagonal or cubic arrays in aqueous or alcohol solutions with rod length in the order of 20–45 nm [57]. Thus, a highly heterogeneous microstructure is expected for supported ultra-thin films, with thickness of the order of the rod length, due to the surface roughness.

In order to test the effect of the substrate on the film microstructure and, consequently, on the water uptake, we performed water sorption measurements in films with thickness around 80 nm on PTFE (using QCM) and glass (using EEP) substrates. The isotherms, also shown in Fig. 5a, indicate that the 66 nm Nafion film deposited on PTFE has similar sorption behaviour as those deposited on gold, while the 81 nm film formed on glass has a higher water sorption but still remain below the sorption values of the bulky membrane.

Using in situ grazing-incidence small-angle X-ray scattering (GISAXS), Weber and coworkers [58] have recently shown that the wetting interaction in the Nafion/substrate interface affects the orientation of ionomer channels for films around 100 nm thick. Hydrophobic surfaces favours ionomer domains oriented parallel to the surface, while films deposited on SiO_2 surfaces exhibit isotropic orientation of the domains, promoting water sorption and swelling. This study demonstrates that the 2D confinement of Nafion thin film restricts the swelling in the out-of-plane direction, and this could be the reason for the lower water sorption observed in our thin Nafion films compared to the bulky unsupported membranes.

As mentioned above, the EEP technique measures the film thickness as a function of the water activity, from which the water uptake is calculated. The film swelling is measured perpendicular to the film surface. In Fig. 5b, the change of thickness for an ultra-thin Nafion film deposited on a glass substrate is depicted. The hysteresis during the sorption and de-sorption steps is very small, indicating that the structural relaxation in the polymer is accomplished during the process. The thickness of the dry film is 81 nm, while the extrapolated thickness of the film at $a_w=1$ is 100 nm, that is, relative thickness change from dryness to water saturation is close to 20%. The observed swelling follows the isotherm pattern of this film plotted in Fig. 5a, calculated using 1.80 g cm^{-3} for the density of dry Nafion. The water sorption of this film calculated using the upper limit density value of 2.0 g cm^{-3} for dry Nafion is also shown in Fig. 5a. It can be seen that the water sorption is independent of the dry Nafion density at low water activities, while it is around 10% lower in the high water activity region, indicating that this choice of density makes the water sorption of the thin Nafion films even much lower in relation to bulk membranes.

The low water sorption and swelling characteristics of Nafion very thin films (<100 nm) should affect other relevant properties for understanding the transport processes in the three phase region of PEM fuel cells. This has been corroborated by studies of proton conduction in Nafion films obtained by spin coating [22] and Nafion adsorption [59]. The decrease of conductivity with decreasing thickness may be due to the hindrance of water sorption and the increased activation energy for proton conduction in the thin films would indicate a change from a Grotthuss to a surface diffusion mechanism as the amount of water in the film nanochannels is reduced by the substrate effect.

3.2. Water sorption of thin Nafion films: Effect of thickness and aging

We have prepared thin Nafion films on glass in order to test the effect of thickness on the water uptake of these supported films. The thickness (dry films) range between 81 and 1028 nm and in all cases the water sorption and swelling were determined by the EEP technique.

The measurements were performed after aging the samples as indicated in Table 1. The results, summarized in Fig. 6, indicate that the water uptake on films aged up to two days (open symbols) are, on average, between 1 and 2 λ units higher than those measured on films aged for periods between 10 and 30 days (grey symbols), all over the range of water activities. The averaged water uptake at $a_w=0.9$, interpolated for the different films, is $\lambda=8.0\pm0.5$ for fresh films (aged up to two days) and $\lambda=7.0\pm0.6$ for those aged 10–30 days. This effect is more clearly shown in the case of samples 4 and 5 (Table 1): A film of dry thickness 534 nm which was measured after 2 days (sample 4) and 30 days aging (sample 5). Although the dry thickness of the film kept almost unchanged, the water uptake at $a_w=0.9$ decreased from $\lambda=8.30$ down to $\lambda=7.25$.

Table 1
Thickness, treatment and water uptake at a_w=0.9 of Nafion thin films deposited on glass.

Sample	Thickness dry film (nm)	Thickness at a_w=1 (nm)	Elongation (%)	Treatment	λ at a_w=0.90
1	81	100	23	Aged 10 days	6.40
2	305	395	30	Aged 2 days	7.55
3	518	655	26	Aged 15 days	6.55
4	534	704	32	Aged 2 days	8.30
5	536	684	28	Aged 30 days	7.25
6	622	788	27	Aged 30 days	7.65
7	663	860	30	Aged 30 days	7.10
8	954	1257	32	–	8.30
9	983	1291	31	–	8.10
10	983	1233	28	Heated 1 h at 60 °C	7.13
11	1028	1377	34	Aged 2 days	7.96

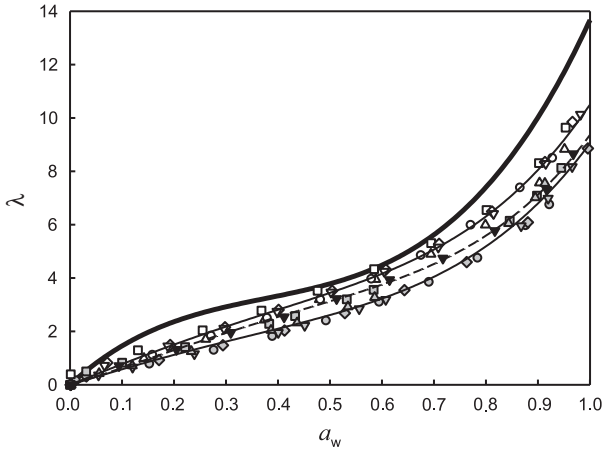

Fig. 6. Water sorption isotherms of thin Nafion films supported on glass determined by EEP, at room temperature, as compared to bulky Nafion (solid line). Open symbols correspond to samples aged up to 2 days, grey symbols to samples aged 10–30 days and closed symbols to the thermically annealed sample 10. Thickness: (○) 81 nm; (Δ) 305 nm; (◇) 518 nm; (□) 534 nm; (■) 534 nm annealed; (▽) 622 nm; (△) 663 nm; (⋄) 954 nm; (∇) 983 nm; (▼) 983 nm thermically annealed; (○) 1028 nm. The thin solid lines correspond to the best fit of the fresh and annealed films, and the dashed line to the best fit of the thermally annealed film.

Sample 10 is the same film as sample 9, measured just after prepared, except that it was heated at 60 °C during 1 h. The results in Fig. 6 (closed symbols) and Table 1 show that this gently thermal annealing produces a decrease in the water uptake, at a_w=0.9, from λ=8.10 to λ=7.13, which is similar to the value obtained with a long aging at room temperature.

In summary, these results on a glass support seem to demonstrate that, contrary to the observed for ultra-thin films supported on gold, there is no thickness effect on the water uptake of supported thin Nafion films. Independently of their thickness, the fresh films uptake more water than those aged for more than 10 days, probably as a consequence of a slow relaxation of the polymer microstructure.

According with the above mentioned GISXAS studies [58], the thermal annealing of Nafion thin films induces the formation of crystalline domains near the substrate interface, reducing the water uptake. Our results would indicate that the increase of Nafion cystallinity induced by thermal annealing could also occur at room temperature by a slow structural relaxation.

A simple experiment was then performed to validate this argue: A Nafion thin film (320 nm) was deposited on a glass substrate and its water sorption was followed during more than 40 days using the EEP technique. The results, shown in Fig. 7, indicate that the water sorption measured at a_w=0.9 decreases almost exponentially, with a relaxation time of approximately six days. Thus, the results described above can be rationalized in terms of the slow polymer relaxation to form crystalline domains, a fact that need to be confirmed, for instance, using the GISAXS technique on samples with different aging treatment.

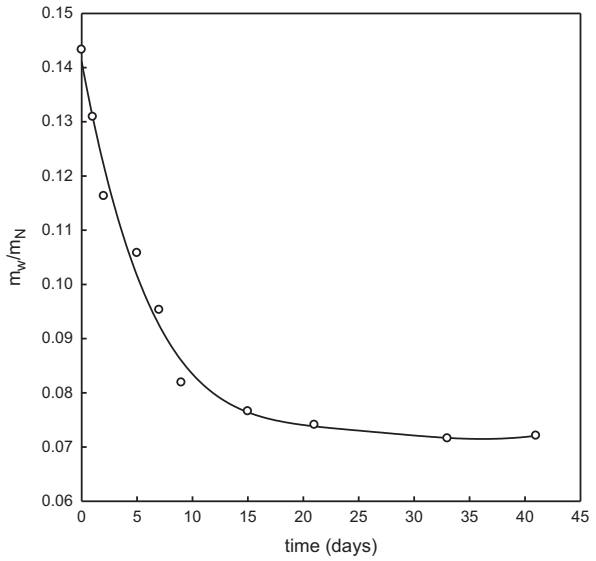

Fig. 7. Water sorption at a_w=0.9 of a Nafion film (dry thickness: 320 nm) deposited on glass as a function of time. The water uptake is expressed as the ratio mass of water (m_w) per mass of dry Nafion (m_N).

The increase of thickness during the water uptake is shown in Table 1. Fresh films at a_w=1 exhibit thickness 32% higher than dry films, while the average elongation for aged films is 28%. Clearly, the film elongation in the direction perpendicular to the surface is related with the water uptake and it is independent on the film thickness.

Thampan et al. [60] reported that the volumetric swelling of bulky Nafion upon hydration is 43%. Film volume increases 14% in the thickness direction, 14% in the lateral axis, and 10% in the extrusion orientation. Nandan et al. [53] measured a 9.5% thickness increase in a bulky Nafion membrane. Our results indicate that the thickness of the supported thin films increases more upon hydration (approximately by a factor 3) than bulky membranes. That is, the restriction to lateral swelling in supported membranes enhances the swelling perpendicular to the substrate, but this unidirectional swelling does not reach the values of the volumetric swelling in bulky membranes. In support of this argument we prepared a Nafion film, ca. 500 nm in thickness, on glass and determined its area using image software (Motic Images Plus 2.0). The glass-supported film was then equilibrated in water vapour (a_w=1) and also immersed in liquid water and its area was determined in each case. The results summarized in Table 2 show that the area expansion upon hydration is lower than 2%.

3.3. Water sorption of thin Nafion films: Effect of the substrate

Table 3 summarizes the thickness of aged dry thin Nafion films deposited on different substrates, along with thickness values upon hydration and the corresponding elongation. Water sorption isotherms are depicted in Fig. 8, where it is seen that water uptake of films deposited on hydrophilic Si and glass surfaces are very similar. On the other hand, the sorption of films over

Table 2
Area expansion upon hydration of a Nafion membrane, 500 nm thick, supported on glass.

Membrane treatment	Area (cm^2)
Dry	1.127 ± 0.001
Equilibrated 15′ in water vapour	1.150 ± 0.004
Equilibrated 30′ in water vapour	1.146 ± 0.006
Inmersed in liquid water	1.142 ± 0.004

Table 3
Thickness, treatment and water uptake at $a_w=0.9$ of Nafion thin films deposited on different substrates.

Substrate	Thickness dry film (nm)	Thickness at $a_w=1$ (nm)	Elongation (%)	Treatment	λ at $a_w=0.90$
Si	396	512	29	Aged 30 days	7.60
Glass	536	684	28	Aged 30 days	7.20
Gold	605	740	22	Aged 10 days	5.75
Graphite	318	372	17	Aged 10 days	4.58
ITO	606	719	19	Aged 40 days	4.32

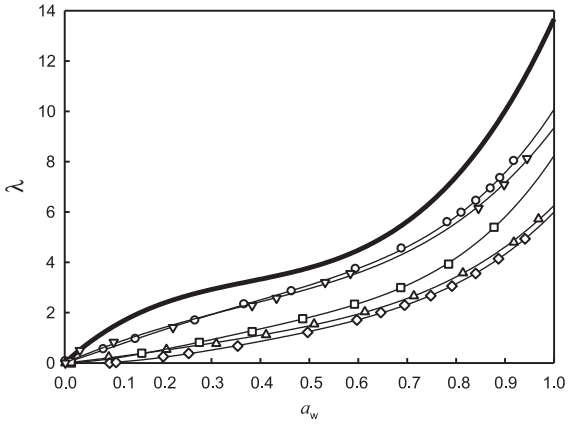

Fig. 8. Water sorption isotherm at room temperature of thin Nafion films, determined by EEP, supported on different substrates as compared to bulky Nafion (solid line): (◇) ITO; (▽) glass; (○) Si; (□) Au; (△) graphite.

hydrophobic graphite and ITO surfaces is much lower, being the sorption on gold supported films intermediate between both types of surfaces. It is interesting to note that the elongation on Si and glass is consistent with the water sorption values.

Nafion's charged side chain is the hydrophilic part of the polymer, being the Teflon-like backbone the hydrophobic one. Neutron reflectrometry studies [61–63] on thin Nafion films have revealed that different layer structures of Nafion exist in contact with glassy carbon and Pt substrates. Hydrophobic or less hydrophilic domains are assumed to form on Pt and glassy carbon, being considered as experimental evidence that the interfacial and long-range structural properties of Nafion are affected by the substrate.

The excess of water uptake by the hydrophilic surfaces as compared to the hydrophobic ones could have two contributions: A higher affinity for water of the Nafion-substrate interfacial region, and a larger extension of the polymer chain when it is attached to the substrate by the hydrophilic charged side chain. The different wetting interactions observed in GISAXS experiments [58] for hydrophobic and hydrophilic substrates, leading to surface-parallel or isotropic orientation of crystalline domains is obviously related with the second contribution.

4. Conclusions

The water uptake by ultra-thin and thin Nafion films with thickness between 17 and 1000 nm were measured on different substrates at room temperature by QCM and EEP techniques. The water uptake, measured as number of water molecules per ionic group in the polymer, is much lower than that observed in bulky Nafion 117 membranes. Water sorption is independent of the film thickness for thin Nafion films (80–1000 nm) supported on glass, but is slightly dependent on the thickness for ultra-thin films supported on gold (QCM experiments). It should also be noted that water sorption determined for the 605-nm thick film supported on gold (Table 3) is higher than that observed in for the ultra-thin films. This behaviour is similar to that observed in a recent QCM study [39] performed at higher temperature (80 °C), but differs significantly from others QCM studies of thin Nafion films reporting either, a water sorption similar to bulky membranes [37], or a very low water uptake [38].

On the other hand, we observed that the water uptake depends on the aging and mainly on the type of substrate. The hydrophilic substrates (Si, glass) show higher water sorption than the hydrophobic ones (graphite, Au, ITO), although all of them sorb less water than bulky membranes. The differences in water uptake between bulk membranes and thin supported films are more evident near $a_w=1$, that is, close to the conditions of interest in PEM fuel cells.

The density of the dry Nafion film reported in the literature varies between 1.80 and 2.00 g cm^{-3} and experimental revision is required in order to validate the water sorption measured by the EEP technique. In this work, we adopted the lower bound density value, which yields to upper limit values for the water sorption. The use of the upper bound would just reinforce the conclusions obtained when comparing thin and bulky films.

The water uptake of thin and ultra-thin films changes with aging. The long aging times required for observing water sorption differences indicate that the relaxation of the backbone and the side chains of the polymer are very slow. The relaxation time, determined by following the water uptake as a function of time, is of the order of days and it seems to be complete for films aged more than 10 days, and could be related with the slow reorientation of crystalline domains, as suggested by GISAXS studies [58].

The film swelling (elongation) in the direction perpendicular to the film, obtained from the ellipsometric data, is much higher than the expansion of bulky membrane upon hydration in the same direction. The elongation is also dependent on the nature of the substrate, but independent of film thickness.

Finally, the relevance of these results in the modelling of the three-phase region of proton exchange membrane fuel cells is worthy of mention. Watanabe et al. [64] studied the effect of Nafion thickness on electrocatalytic properties for hydrogen oxidation and oxygen reduction on Nafion-coated Pt electrodes. It was found that a Nafion film thickness lower than 200 nm is required to avoid the diffusion of the reactant gases to catalyst sites being the rate-determining step. This critical thickness is within the range of the Nafion nanofilms studied here, although the film thickness was estimated using the density of dry Nafion.

Continuous microscopic [65] (including Schroeder's paradox) and multiscale [66] irreversible thermodynamics models of transport processes in an electrochemical fuel cell interface, use

essentially sorption parameters of bulky Nafion, and they are expected to overestimate the hydration level of Nafion in the three-phase region.

It has been also shown by molecular dynamics (MD) simulation of a model polymer–catalyst–carbon interface, [67] that the diffusion of water and oxygen in the thin Nafion layer covering the catalyst particles varies according to the contribution of different mechanisms, whose relative weights are a function of the water content, which was fixed by the authors with values typical of bulky Nafion membranes. On the other hand, MD simulations aiming to determine the water content dependence of the critical size of the gap between a catalyst nanoparticle and the Nafion membrane for proton conduction, [68] should also rely on sorption data on nanosized Nafion films, as those present in the three-phase region and studied in this work.

Acknowledgments

The authors acknowledge the financial support from ANPCyT (PAE 36985, PAE-37063-PME-2006-00038 and PICT 2010-00026) and CONICET (PIP 00095). HRC and MCF are members of the Consejo Nacional de Investigaciones Científicas y Técnicas (CONICET).

References

[1] K.A. Mauritz, R.B. Moore, State of understanding of Nafion, Chem. Rev. 104 (2004) 4535–4583.
[2] T.D. Gierke, G.E. Munn, F.C. Wilson, The morphology in Nafion perfluorinated membrane products, as determined by wide- and small-angle x-ray studies, J. Polym. Sci. Polym. Phys. 19 (1981) 1687–1704.
[3] E.J. Roche, M. Pineri, R. Duplessix, A.M. Levelut, Small-angle scattering studies of Nafion membranes, J. Polym. Sci. Polym. Phys. 19 (1981) 1–11.
[4] A. Eisenberg, H.L. Yeager, Perfluorinated Ionomer Membranes, ACS Books, Washington, 1982.
[5] M. Fujimura, T. Hashimoto, H. Kawai, Small-angle x-ray scattering study of perfluorinated ionomer membranes. 2. Models for ionic scattering maximum, Macromolecules 14 (1981) 1309–1315.
[6] P.J. James, J.A. Elliott, T.J. McMaster, J.M. Newton, A.M.S. Elliott, S. Hanna, M.J. Miles, Hydration of Nafion® studied by AFM and X-ray scattering, J. Mater. Sci. 35 (2000) 5111–5119.
[7] K. Schmidt-Rohr, Q. Chen, Parallel cylindrical water nanochannels in Nafion fuel-cell membranes, Nat. Mater. 7 (2008) 75–83.
[8] S. Litster, G. McLean, PEM fuel cell electrodes, J. Power Sources 130 (2004) 61–76.
[9] E.A. Ticianelli, C.R. Derouin, A. Redondo, S. Srinivasan, Methods to advance technology of proton exchange membrane fuel cells, J. Electrochem. Soc. 135 (1988) 2209–2214.
[10] S.J. Lee, S. Mukerjee, J.e McBreen, Y.W. Rho, Y.T. Kho, T.H. Lee, Effects of Nafion impregnation on performances of PEMFC electrodes, Electrochim. Acta 43 (1998) 3693–3701.
[11] M.S. Wilson, Membrane catalyst layer for fuel cells, U.S. Pat. 234 (5) (1993) 777.
[12] M.S. Wilson, S. Gottesfeld, Thin-film catalyst layers for polymer electrolyte fuel cell electrodes, J. Appl. Electrochem. 22 (1992) 1–7.
[13] M.S. Wilson, J.A. Valerio, S. Gottesfeld, Low platinum loading electrodes for polymer electrolyte fuel-cells fabricated using thermoplastic ionomers, Electrochim. Acta 40 (1995) 355–363.
[14] M. Carmo, A.R. dos Santos, J.G.R. Poco, M. Linardi, Physical and electrochemical evaluation of commercial carbon black as electrocatalysts supports for DMFC applications, J. Power Sources 173 (2007) 860–866.
[15] R. Subbaraman, D. Strmcnik, V. Stamenkovic, N.M. Markovic, Three phase interfaces at electrified metal-solid electrolyte systems 1. Study of the Pt(*h k l*)-Nafion interface, J. Phys. Chem. C 114 (2010) 8414–8422.
[16] A.A. Franco, Y. Suzue, R.F. de Morais, A. Kachmar, T. Mashio, A. Ohma, K. Shinohara, Multiscale modeling of electrochemical double layer formation on Pt electrodes covered by Nafion. In: 221st ECS Meeting, Abstract 226 (2012).
[17] T. Mashio, K. Malek, M. Eikerling, A. Ohma, H. Kanesaka, K. Shinohara, Molecular dynamics study of ionomer and water adsorption at carbon support materials, J. Phys. Chem. C 114 (2010) 13739–13745.
[18] A. Ohma, T. Mashio, K. Sato, H. Iden, Y. Ono, K. Sakai, K. Akisuki, S. Takaichi, K. Shinohara, Analysis of proton exchange membrane fuel cell catalyst layers for reduction of platinum loading at Nissan, Electrochim. Acta 56 (2011) 10832–10841.
[19] K. Malek, A.A. Franco, Microstructure-based modelling of aging mechanisms in catalyst layers of polymer electrolyte fuel cells, J. Phys. Chem. B 115 (2011) 8088–8101.
[20] D. Damasceno Borges, S. Mossa, K. Malek, G. Gebel, A.A. Franco, Effect of surface hydrophilicity on the formation of Nafion thin film inside PEMFC catalyst layer: a computational study. In: 221st ECS Meeting, Abstract 1098 (2012).
[21] H. Iden, A. Ohma, K. Shinohara, Analysis of proton transport in pseudo catalyst layers, J. Electrochem. Soc. 156 (2009) B1078–B1084.
[22] Z. Siroma, R. Kakitsubo, N. Fujiwara, T. Ioroi, S. Yamazaki, K. Yasuda, Depression of proton conductivity in recat Nafion film measured on flat substrate, J. Power Sources 189 (2009) 994–998.
[23] D.R. Morris, X. Sun, Water-sorption and transport properties of Nafion 117, J. Appl. Polym. Sci. 50 (1991) 1445–1452.
[24] R. Duplessix, M. Escoubes, B. Rodmacq, F. Volino, E. Roche, A. Eisemberg, M. Pineri, In water in polymers, in: S.P. Rowland (Ed.), ACS Symposium Series No 127, American Chemical Society, Washington DC, 1980, p. 469.
[25] K.K. Pushpa, D. Nandan, R.M. Iyer, Thermodynamics of water sorption by perfluorosulphonate (Nafion-117) and polyestirene–divinylbenzene sulphonate (Dowex 50 W) ion-exchange resins at 298 ± 1 K, J. Chem. Soc. Faraday Trans. I 84 (1988) 2047–2056.
[26] T.A. Zawodzinski Jr., M. Neeman, L.O. Sillerud, S. Gottesfeld, Determination of water diffusion coefficients in perfuorosulfonate ionomeric membranes, J. Phys. Chem. 95 (1991) 6040–6044.
[27] T.A. Zawodzinski Jr., C. Derouin, S. Radzinski, R.J. Sherman, V.T. Smith, T.E. Springer, S. Gottesfeld, Water uptake by and transport through Nafion 117 membranes, J. Electrochem. Soc. 140 (1993) 1041–1047.
[28] D. Rivin, C.E. Kendrick, P.W. Gibson, N.S. Schneider, Solubility and transport behavior of water and alcohols in Nafion, Polymer 42 (2001) 623–635.
[29] M. Miyake, J.S. Wainright, R.F. Savinell, Evaluation of a sol–gel derived Nafion/Silica hybrid membrane for proton electrolyte membrane fuel cell applications. I. Proton conductivity and water content, J. Electrochem. Soc. 148 (2001) A898–A904.
[30] M. Legras, Y. Hirata, Q.T. Nguyen, D. Langevin, M. Métayer, Sorption and diffusion behaviors of water in Nafion 117 membrane with different counter-ions, Desalination 147 (2002) 351–357.
[31] P.J. Reucroft, D. Rivin, N.S. Schneider, Thermodynamics of Nafion–vapor interactions. I. Water vapor, Polymer 43 (2002) 5157–5161.
[32] D.J. Burnett, A.R. Garcia, F. Thielmann, Measuring moisture sorption and diffusion kinetics on proton exchange membranes using a gravimetric vapor sorption apparatus, J. Power Sources 160 (2006) 426–430.
[33] H. Takata, N. Mizuno, M. Nishikawa, S. Fukada, M. Yoshitake, Adsorption properties of water vapor on sulfonated perfluoropolymer membranes, Int. J. Hydrogen Energy 32 (2007) 371–379.
[34] J.T. Hinatsu, M. Mizuhata, H. Takenaka, Water uptake of perfluorosulfonic acid membranes from liquid water and water vapor, J. Electrochem. Soc. 141 (1994) 1493–1498.
[35] A. Steck, H.L. Yeager, Water sorption and cation-exchange selectivity of a perfluorosulfonate ion-exchange polymer, Anal. Chem. 52 (1980) 1215–1218.
[36] T.A. Zawodzinski Jr., T.E. Springer, J. Davey, R. Jestel, C. Lopez, J. Valerio, S. Gottesfeld, A comparative study of water uptake by and transport through ionomeric fuel cell membranes, J. Electrochem. Soc. 140 (1993) 1981–1985.
[37] P. Krtil, A. Trojánek, Z. Samec, Kinetics of water sorption in Nafion thin films—quartz crystal microbalance study, J. Phys. Chem. B 105 (2001) 7979–7983.
[38] Y. Yamamoto, M.C. Ferrari, M. Giacinti Baschetti, M.G. De Angelis, G.C. Sarti, A quartz crystal microbalance study of water vapor sorption in a short side-chain PFSI membrane, Desalination 200 (2006) 636–638.
[39] A. Kongkanand, Interfacial water transport measurements in Nafion thin films using quartz-crystal microbalance, J. Phys. Chem. C 115 (2011) 11318–11325.
[40] M. Lee, M. Uchida, H. Yano, D. Tryk, H. Uchida, M. Watanabe, New evaluation method for the effectiveness of platinum/carbon electrocatalysts under operating conditions, Electrochim. Acta 55 (2010) 8504–8512.
[41] Y. Liu, J. Jorne, W. Gu, Thin shell model for proton conduction in PEM fuel cell cathodes, J. Electrochem. Soc. 157 (2010) B1068–B1071.
[42] G.C. Abuin, P. Nonjola, E.A. Franceschini, F.H. Izraelevitch, M.K. Mathe, H.R. Corti, Characterization of an anionic-exchange membranes for direct methanol alkaline fuel cells, Int. J. Hydrogen Energy 35 (2010) 5849–5854.
[43] L.A. Diaz, G.C. Abuin, H.R. Corti, Methanol sorption and permeability in Nafion and acid-doped PBI and ABPBI membranes, J. Membr. Sci. 411-412 (2012) 35–44.
[44] G. Sauerbrey, Verwendung von Schwingquarzen zur Wägung dünner Schichten und zur Mikrowägung, Z. Phys. 155 (1959) 206–222.
[45] M.R. Baklanov, K.P. Mogilnikov, V.G. Polovinkin, F.N. Dultsev, Determination of pore size distribution in thin films by ellipsometric porosimetry, J. Vac. Sci. Technol. B 18 (2000) 1385–1391.
[46] H.G. Tompkins, W.A. McGahan, Spectroscopic Ellipsometry and Reflectometry–A User's Guide, Wiley Interscience, 1999.
[47] M.C. Fuertes, S. Colodrero, G. Lozano, A. Rodríguez González-Elipe, D. Grosso, C. Boissière, C. Sánchez, G.J.A.A. Soler-Illia, H. Míguez, Sorption properties of mesoporous multilayer thin films, J. Phys. Chem. C 112 (2008) 3157–3163.

[48] C. Boissière, D. Grosso, S. Lepoutre, L. Nicole, A. Brunet-Bruneau, C. Sánchez, Porosity and mechanical properties of mesoporous thin films assessed by environmental ellipsometric porosimetry, Langmuir 21 (2005) 12362–12371.
[49] A. Bourgeois, A.B. Bruneau, S. Fisson, B. Demarets, D. Grosso, F. Cagnol, C. Sanchez, J. Rivory, Determination of pore size distribution in thin organized mesoporous silica films by spectroscopic ellipsometry in the visible and infrared range, Thin Solid Films 447-448 (2004) 46–50.
[50] Q. Zhao, P. Majsztrik, J. Benziger, Diffusion and interfacial transport of water in Nafion, J. Phys. Chem. B 115 (2011) 2717–2727.
[51] L.A. Zook, J. Leddy, Density and solubility of Nafion: recast, annealed, and commercial films, Anal. Chem. 68 (1996) 3793–3796.
[52] K.J. Oberbroeckling, D.C. Dunwoody, S.D. Minteer, J. Leddy, Density of Nafion exchanged with transition metal complexes and tetramethyl ammonium, ferrous, and hydrogen ions: commercial and recast films, Anal. Chem. 74 (2002) 4794–4799.
[53] D. Nandan, H. Mohan, R.M. Iyer, Methanol and water uptake, densities, equivalental volumes and thicknesses of several uni- and divalent ionic perfluorosulphonate exchange membranes (Nafion-117) and their methanol–water fractionation behaviour at 298 K, J. Membr. Sci. 71 (1992) 69–80.
[54] W. Paik, T.E.W. Springer, S. Srinivasan, Kinetics of fuel cell reactions at the platinum/solid polymer electrolyte interface, J. Electrochem. Soc. 136 (1989) 644–649.
[55] N. Pantelić, C.M. Wansapura, W.R. Heineman, C.J. Seliskar, Dynamic in situ spectroscopic ellipsometry of the reaction of aqueous iron(II) with 2,2′-bipyridine in a thin Nafion film, J. Phys. Chem. B 109 (2005) 13971–13979.
[56] P. Schroeder, Uber Erstarrungs – und Quellungsercheinungen von Gelatine, Z. Phys. Chem. 45 (1903) 75–117.
[57] P. Aldebert, B. Dreyfus, M. Pineri, Small-angle neutron scattering of perfluorinated ionomers in solution, Macromolecules 19 (1986) 2651–2653.
[58] M.A. Modestino, A. Kusoglu, A. Hexemer, A.Z. Weber, R.A. Segalman, Controlling Nafion structure and properties via wetting interactions, Macromolecules 45 (2012) 4681–4688.
[59] D.K. Paul, A. Fraser, K. Karan, Towards the understanding of proton conduction mechanism in PEMFC catalyst layer: conductivity of adsorbed Nafion films, Electrochem. Commun. 13 (2011) 774–777.
[60] T. Thampan, S. Malhotra, H. Tang, R. Datta, Modelling of conductive transport in proton-exchange membranes for fuel cells, J. Electrochem. Soc. 147 (2000) 3242–3250.
[61] D.L. Wood 3rd, J. Chlistunoff, J. Majewski, R.L. Borup, Nafion structural phenomena at platinum and carbon interfaces, J. Am. Chem. Soc. 131 (2009) 18096–18104.
[62] V.S. Murthi, J.A. Dura, S. Satija, C.F. Majkrzak, Water uptake and interfacial structural changes of thin film Nafion membranes measured by neutron reflectivity for PEM fuel cells, ECS Trans. 16 (2008) 1471–1485.
[63] J.A. Dura, V.S. Murthi, M. Hartman, S. Satija, C.F. Majkrzak, Multilamellar interface structures in Nafion, Macromolecules 42 (2009) 4769–4774.
[64] M. Watanabe, H. Igarashi, K. Yosioka, An experimental prediction of the preparation condition of Nafion-coated catalyst layers for PEFCs, Electrochim. Acta 40 (1995) 329–334.
[65] A.Z. Weber, J. Newman, Transport in polymer-electrolyte membranes: I. Physical Model, J. Electrochem. Soc. 150 (2003) A1008–A1015.
[66] A.A. Franco, P. Schott, C. Jallut, B. Maschke, A dynamic mechanistic model of an electrochemical interface, J. Electrochem. Soc. 153 (2006) A1053–A1061.
[67] E.J. Lamas, P.B. Balbuena, Molecular dynamics studies of a model polymer–catalyst–carbon interface, Electrochim. Acta 51 (2006) 5904–5911.
[68] J. Liu, M.E. Selvan, S. Cui, B.J. Edwards, D.J. Keffer, W.V. Steele, Molecular-level modeling of the structure and wetting of electrode/electrolyte interfaces in hydrogen fuel cells, J. Phys. Chem. C 112 (2008) 1985–1993.